

# Integrin-Mediated Interactions Control Macrophage Polarization in 3D Hydrogels

Byung-Hyun Cha, Su Ryon Shin, Jeroen Leijten, Yi-Chen Li, Sonali Singh, Julie C. Liu, Nasim Annabi, Reza Abdi, Mehmet R. Dokmeci, Nihal Engin Vrana, Amir M. Ghaemmaghami, and Ali Khademhosseini\*

Adverse immune reactions prevent clinical translation of numerous implantable devices and materials. Although inflammation is an essential part of tissue regeneration, chronic inflammation ultimately leads to implant failure. In particular, macrophage polarity steers the microenvironment toward inflammation or wound healing via the induction of M1 and M2 macrophages, respectively. Here, this paper demonstrates that macrophage polarity within biomaterials can be controlled through integrin-mediated interactions between human monocytic THP-1 cells and collagen-derived matrix. Surface marker, gene expression, biochemical, and cytokine profiling consistently indicate that THP-1 cells within a biomaterial lacking cell attachment motifs yield proinflammatory M1 macrophages, whereas biomaterials with attachment sites in the presence of interleukin-4 (IL-4) induce an anti-inflammatory M2-like phenotype and propagate the effect of IL-4 in induction of M2-like macrophages. Importantly, integrin  $\alpha 2\beta 1$  plays a pivotal role as its inhibition blocks the induction of M2 macrophages. The influence of the microenvironment of the biomaterial over macrophage polarity is further confirmed by its ability to modulate the effect of IL-4 and lipopolysaccharide, which are potent inducers of M2 or M1 phenotypes, respectively. Thus, this study represents a novel, versatile, and effective strategy to steer macrophage polarity through integrin-mediated 3D microenvironment for biomaterial-based programming.

## 1. Introduction

Inflammation is an inevitable consequence of implantation and is closely linked to the implant's clinical outcome. Upon implantation, immune cells migrate to the implantation site and initiate a localized inflammatory response.<sup>[1]</sup> Although inflammation is an indispensable element in tissue regeneration, an intense or chronic inflammatory response will significantly limit natural healing. Moreover, detrimental inflammatory responses can result in fibrotic capsule formation around the implant and ultimately result in failure of the implants.<sup>[1b]</sup> Thus, the ability to actively control inflammation in regenerating tissues and implanted medical devices represents a major yet unsolved challenge.

Among the variety of immune cells, monocytes and macrophages play a particularly critical role that determines successful tissue-implant integration or implant failure.<sup>[2]</sup> Specifically, macrophage polarity strongly influences clinical

Dr. B.-H. Cha, Dr. S. R. Shin, Dr. J. Leijten, Dr. Y.-C. Li, Dr. S. Singh, Dr. J. C. Liu, Dr. N. Annabi, Dr. R. Abdi, Dr. M. R. Dokmeci, Dr. N. E. Vrana, Dr. A. M. Ghaemmaghami, Dr. A. Khademhosseini  
Biomaterials Innovation Research Center  
Department of Medicine  
Brigham and Women's Hospital  
Harvard Medical School  
Cambridge, MA 02139, USA  
E-mail: alik@bwh.harvard.edu

Dr. B.-H. Cha, Dr. S. R. Shin, Dr. J. Leijten, Dr. Y.-C. Li, Dr. S. Singh, Dr. J. C. Liu, Dr. N. Annabi, Dr. R. Abdi, Dr. M. R. Dokmeci, Dr. N. E. Vrana, Dr. A. M. Ghaemmaghami, Dr. A. Khademhosseini  
Harvard-MIT Division of Health Sciences and Technology  
Massachusetts Institute of Technology  
Cambridge, MA 02139, USA

Dr. B.-H. Cha, Dr. S. R. Shin, Dr. Y.-C. Li, Dr. M. R. Dokmeci, Dr. A. Khademhosseini  
Wyss Institute for Biologically Inspired Engineering  
Harvard University  
Boston, MA 02115, USA

Dr. J. Leijten  
Department of Developmental BioEngineering  
MIRA Institute for Biomedical Technology and Technical Medicine  
University of Twente  
7500 AE Enschede, The Netherlands

Dr. S. Singh, Dr. A. M. Ghaemmaghami  
Division of Immunology  
School of Life Sciences  
Faculty of Medicine and Health Sciences  
University of Nottingham  
Nottingham, NG7 2RD, UK

Dr. J. C. Liu  
Davidson School of Chemical Engineering and Weldon  
School of Biomedical Engineering  
Purdue University  
West Lafayette, IN 47907, USA

Dr. N. Annabi  
Department of Chemical Engineering  
Northeastern University  
Boston, MA 02115, USA

DOI: 10.1002/adhm.201700289

outcome through the balance between proinflammatory M1 and regenerative M2 macrophages. Classically activated M1 macrophages are associated with a proinflammatory response.<sup>[3]</sup> By contrast, alternatively activated M2 macrophages are associated with an anti-inflammatory response, which induces angiogenesis and proliferation.<sup>[3b,4]</sup> Therefore, harnessing macrophage polarity presents a unique opportunity to control inflammation, prevent rejection, and accelerate integration of biomaterials and medical devices.

Macrophage polarization is most commonly controlled via exposure to biochemical factors. Specifically, the M1 macrophage phenotype is typically induced through interferon gamma (IFN $\gamma$ ) or lipopolysaccharide (LPS) stimulation, while the M2 macrophage phenotype is typically induced through interleukin-4 (IL-4) or interleukin-13 (IL-13) stimulation.<sup>[5]</sup> However, these approaches are not easily translated into in vivo approaches due to the challenge of delivery, temporal nature of the stimulus, and risk of adverse effects.

Recent advances in biomaterials science have identified that a biomaterial's design can be leveraged to instruct the host's immune system.<sup>[6]</sup> For example, novel biomaterial surfaces,<sup>[7]</sup> improved immune-instructive biomaterials,<sup>[8]</sup> and incorporating immune modulating cells (e.g., stem cells)<sup>[9]</sup> could influence the wound healing process. Within the same context, there are several studies in which the phenotype of macrophages inside different 3D biomaterial environments has been studied.<sup>[10]</sup> In addition, several physical factors have recently been reported to regulate macrophage polarization.<sup>[11]</sup> These factors include biomaterial pore size,<sup>[12]</sup> mechanical stimulation,<sup>[13]</sup> and extracellular matrix proteins (ECM)<sup>[14]</sup> among others. However, the underlying mechanisms of how biomaterials steer macrophage polarity has remained poorly understood. This has obscured the underlying biomaterial design principles, which has limited our capability to engineer smart biomaterials with the ability to steer macrophage polarity.

Cell adhesion plays an integral role in enabling communication between cells and their microenvironment. This form of interaction is known to regulate numerous aspects of cellular behavior including migration, proliferation, morphogenesis, and differentiation.<sup>[15]</sup> It is well established that surface structure, pore size, and ECM influence a cell's ability to adhere to substrates through integrin interactions.<sup>[16]</sup> Indeed, integrins are well known to influence inflammation<sup>[17]</sup> and fibrosis.<sup>[18]</sup> However, their role in monocyte to macrophage differentiation and particularly macrophage polarization is yet to be fully

understood. Here, we hypothesized that integrin-mediated cell–biomaterial interactions could play a key role in macrophage polarization. Given that in vivo these events take place in the context of ECM and in 3D, obtaining a clear understanding of the role of integrins in macrophage polarization in a 3D microenvironment will be more physiologically relevant than in a 2D environment.<sup>[19]</sup> Therefore, in this study, we have used two distinct hydrogel systems to probe the effect of cell–biomaterial interactions on macrophage polarization in a 3D environment. Specifically, we have set out to investigate whether macrophage polarity can be controlled through integrin-mediated biomaterial-based programming.

## 2. Results and Discussion

### 2.1. Characterization of Two Distinct Monocyte Laden 3D Hydrogels

The effect of 3D biomaterial environment on monocyte behavior has remained largely unknown. We therefore explored the behavior of human monocytic THP-1 cells encapsulation in two distinct hydrogel systems, namely, gelatin methacryloyl (GelMA) and poly(ethylene glycol) diacrylate (PEGDA).

First, we investigated the microenvironment as presented by GelMA by varying the polymer concentrations from 5% to 15% (w/v). Increasing the GelMA concentration from 5% to 15% (w/v) increased the hydrogel's crosslinking density and compressive modulus due to an inverse relation between the GelMA concentration and its porosity, as previously described by our group.<sup>[20]</sup> In particular, the compressive modulus increased from  $3.0 \pm 0.3$  to  $25.8 \pm 1.5$  kPa (Figure S1, Supporting Information). Upon encapsulation, THP-1 cells in the softer 5% GelMA hydrogels demonstrated significantly higher levels of cell survival (Figure S2A,B, Supporting Information) as well as increased metabolic activities compared to those encapsulated in the stiffer 10% and 15% GelMA hydrogels (Figure S3, Supporting Information). In addition, the swelling characteristics of a hydrogel are important in its biocompatibility through affecting various parameters including mass transport and mechanical properties.<sup>[21]</sup> We performed a swelling test for GelMA hydrogels at various concentrations. The 5% GelMA hydrogels had significantly higher levels of swelling ratio compared to the 10% and 15% GelMA hydrogels. The low cell viability and metabolic activities of THP-1 cells within both 10%

Dr. R. Abdi  
Transplant Research Center  
Renal Division  
Brigham and Women's Hospital and Children's Hospital  
Boston, MA 02115, USA

Dr. N. E. Vrana  
Fundamental Research Unit  
Protip Medical  
8 Place de l'Hôpital 67000 Strasbourg, France

Dr. N. E. Vrana  
Institut National de la Santé et de la Recherche Médicale (INSERM)  
UMR-S 1121  
"Biomatériaux et Bioingénierie"  
11 rue Humann 67085 Strasbourg Cedex, France

Prof. A. Khademhosseini  
Department of Bioindustrial Technologies  
College of Animal Bioscience and Technology  
Konkuk University  
Seoul 143-701, Republic of Korea

Prof. A. Khademhosseini  
Nanotechnology Center  
King Abdulaziz University  
Jeddah 21569, Saudi Arabia

 The ORCID identification number(s) for the author(s) of this article can be found under <https://doi.org/10.1002/adhm.201700289>.

and 15% (w/v) GelMA can be explained by increased stiffness values and reduced swelling ratio when using relatively high (w/v) amounts of GelMA. These results underlined THP-1 cells' sensitivity to their microenvironment's physical properties (e.g., stiffness and mass transport) which could in turn impact the biological processes (Figure S4, Supporting Information). In line with our finding, it has previously been reported that the stiffness of 2D hydrogels correlates with the number of monocytes that are differentiated into macrophages.<sup>[22]</sup> Based on our results, all subsequent experiments were performed with 5% (w/v) GelMA.

Monocytes can be chemically driven into a regenerative M2 macrophage phenotype through exposure to IL-4.<sup>[23]</sup> Analysis of release kinetics demonstrated that GelMA acted as a proper cytokine reservoir with a sustained release of IL-4 over 7 d (Figure S5, Supporting Information). Even though macrophages are highly plastic and can show phenotypic changes within hours; the differentiation or induction in *in vitro* conditions is typically done for 6–8 d. Future studies could focus on better understanding of the kinetics of the observed phenotypical changes.<sup>[24]</sup> Thus the IL-4 release profiles from the hydrogel provide an ample time window to present monocytes with a microenvironment that is conducive to macrophage polarization.

Although GelMA appeared highly suitable to study macrophage polarization within a 3D environment, we simultaneously explored a distinct second hydrogel system (10% (w/v) PEGDA) to exclude possible biomaterial-based bias. To maximize the similarities between the two hydrogel systems, we matched the compressive modulus of 10% (w/v) PEGDA to that of 5% GelMA (Figure S6, Supporting Information) and minimized the differences in IL-4 release (Figure S7, Supporting Information). However, the two hydrogel systems remained inherently distinct in that unlike PEGDA, GelMA contains cell attachment sites.

THP-1 cells were used as a surrogate for human monocytes to ensure reproducibility of our findings by eliminating potential donor-to-donor variation. Monocytic cells were encapsulated in PEGDA and GelMA hydrogels with or without IL-4 incorporation to examine their morphological phenotype over 6 d. Intriguingly, the size of the THP-1 cells in GelMA hydrogels became progressively larger (Figure 1A). Supplementation of IL-4 to GelMA hydrogels further exacerbated this cell enlargement. By contrast, the size of the THP-1 cells in PEGDA hydrogels remained the same under all conditions and time points. Quantitative analysis of the cell diameters confirmed that cells within GelMA ( $15.6 \pm 0.6 \mu\text{m}$ ) and IL-4 incorporated GelMA ( $20.3 \pm 0.9 \mu\text{m}$ ) hydrogels became significantly larger than cells within PEGDA ( $10.0 \pm 0.3 \mu\text{m}$ ) and IL-4 incorporated PEGDA ( $10.4 \pm 0.4 \mu\text{m}$ ) after 6 d of culture (Figure 1B). Cell size distribution analysis revealed that while GelMA hydrogels created a shift in the general cell size population, IL-4 yielded an additional enrichment of the largest cell fraction (Figure 1C). Taken together, GelMA hydrogel's bioactive microenvironment influenced the THP-1 cells' shape, whereas the bioinert microenvironment of PEGDA did not. Thus, hydrogel composition has been found to play a significant role on the size of the encapsulated THP-1 cells. Even though no previous study has definitively demonstrated the effect of monocyte size on macrophage polarity, it is well documented that cell size and cell shape<sup>[25]</sup>

are important determinants of cellular events including differentiation, function, proliferation, and apoptosis.<sup>[26]</sup>

## 2.2. Hydrogel Composition Strongly Affects Expression of M1–M2 Macrophage Surface Markers

Next, we set out to determine whether the observed differences in cell size between hydrogel systems correlated with a change in macrophage polarity. To this end, the expression of M1–M2 macrophage surface markers on human monocytic THP-1 cell cultured in PEGDA or GelMA hydrogels was visualized in the presence or absence of IL-4, the M2 macrophage inducing agent (Figure 1D). The well-established surface biomarkers CD86 and CD206 were chosen to identify M1 and M2 macrophages, respectively.<sup>[27]</sup> Semiquantitative image analysis demonstrated that after 6 d, THP-1 cells in GelMA expressed a notably high level of CD206 as well as less intense yet detectable levels of CD86 (Figure 1E). As expected, incorporation of IL-4 in GelMA hydrogels drove the induction of M2 macrophages as evidenced by increasing CD206 and decreasing CD86 expressions. In sharp contrast, THP-1 cells in PEGDA hydrogels expressed high levels of CD86 whereas the CD206 levels were undetectable. Surprisingly, incorporation of IL-4 in PEGDA did not alter the expression of either CD86 or CD206.

To further confirm the observed effects of PEGDA and GelMA hydrogels on macrophage polarity, we fingerprinted the THP-1 cells by profiling their M1–M2 gene expression. Indeed, encapsulation of THP-1 cells in PEGDA resulted in increased expression of the genes encoding M1 inducing transcription factor interferon regulatory factor 5 (*IRF5*) and M1-related cytokine *IL6*, whereas mRNA levels of *IRF5* and *IL6* remained unaffected when cells were encapsulated in GelMA hydrogels (Figure 1F). Furthermore, human monocytic THP-1 cells encapsulated in GelMA hydrogels demonstrated increased gene expression of M2-related cytokine *IL10* expression (Figure 1G).<sup>[28]</sup> Similar to our CD86 observations, the incorporation of IL-4 in PEGDA hydrogels was unable to significantly increase *IL10* and M2 inducing transcription factor signal transducer and activator of transcription 6 (*STAT6*) expression levels, whereas IL-4 incorporated GelMA hydrogels strongly increased their gene expression. Collectively, these results supported the stipulation that a biomaterial's composition can prime monocytes toward either an M1 or an M2 phenotype.

By extension, it might therefore be possible to program the immune system to either pro- or anti-inflammatory responses purely based on the design of a biomaterial. In particular, IL-4 incorporated GelMA hydrogels induce regenerative M2 macrophages, whereas IL-4 incorporated PEGDA hydrogels induced proinflammatory M1 macrophages. PEGDA hydrogel's M1 phenotype inducing effect is further underlined by its ability to block IL-4's capacity to induce M2 macrophages. This is in line with recent studies showing that bioinert PEGDA hydrogels can elicit strong immune response.<sup>[29]</sup> This observation is of interest as poly(ethylene glycol) (PEG) is typically used for its immune-shielding properties, which is based on its mesh size and bioinert nature.<sup>[30]</sup> Regardless, recent studies are in line with our observation that the bioinert PEGDA can elicit a strong immune response.<sup>[29]</sup> Consequently, by understanding

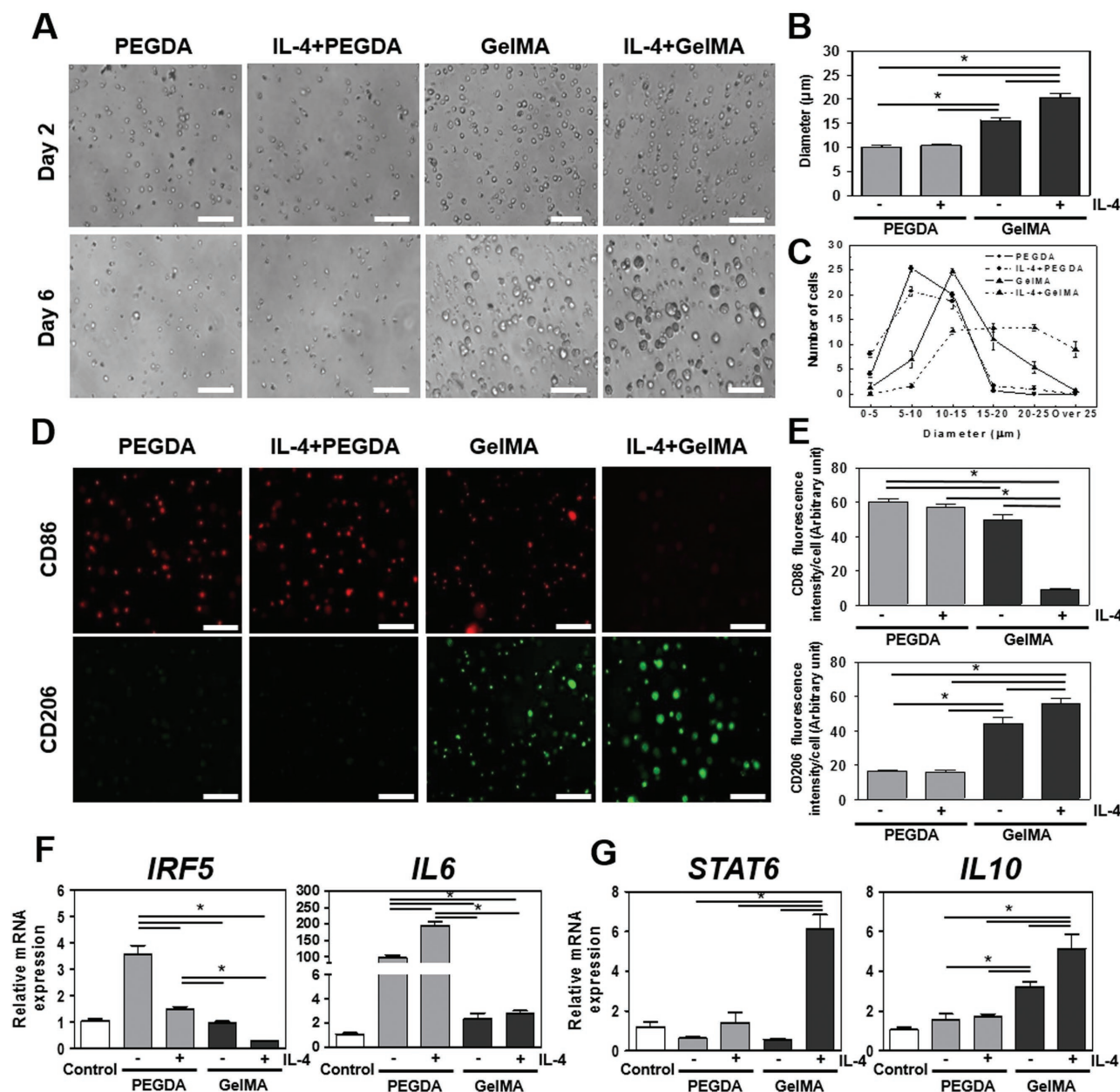


**Figure 1.** Characterization of 3D encapsulated human monocyte THP-1 cells behavior in IL-4 incorporated PEGDA and GelMA hydrogels for 6 d. A) THP-1 cell morphology in IL-4 cytokine incorporated PEGDA and GelMA hydrogels. B) Quantitation of cell diameter in IL-4 cytokine incorporated PEGDA or GelMA hydrogel. C) Distribution of cell diameter in IL-4 cytokine incorporated PEGDA and GelMA hydrogels. D) Images of cells in hydrogel constructs stained for M1 surface marker CD86 (red) and M2 surface marker CD206 (green). Scale bar represents 100 µm. E) Quantitative analysis of images. F) Real-time PCR of M1-related *IRF5* and *IL6* and G) M2-related *STAT6* and *IL10*. Scale bar represents 100 µm. The data are shown as the mean ± SEM (\*,  $p < 0.05$ ).

how biomaterials affect macrophage polarity, we might improve our capability to design biomaterials with improved immunomodulatory properties.

### 2.3. Hydrogel Composition Controls Macrophage's Functional Properties

We then set out to confirm that the PEGDA hydrogel indeed robustly drives THP-1 cells into a functional M1 macrophage

phenotype. To this end, we determined the expression of nitric oxide synthase 2 (*NOS2*), nuclear factor kappa beta (*NFKB*), and tumor necrosis factor alpha (*TNFA*) (Figure 2A) as well as nitrite production (Figure 2B), which are all indicative of M1 functionality. Human monocyte THP-1 cells encapsulated in PEGDA hydrogels demonstrated higher expression levels for all four proinflammatory markers compared to cells encapsulated in GelMA hydrogels. Interestingly, GelMA also guided the proinflammatory response in the absence of IL-4, as noted by increased *NOS2* and *NFKB* expressions compared to the

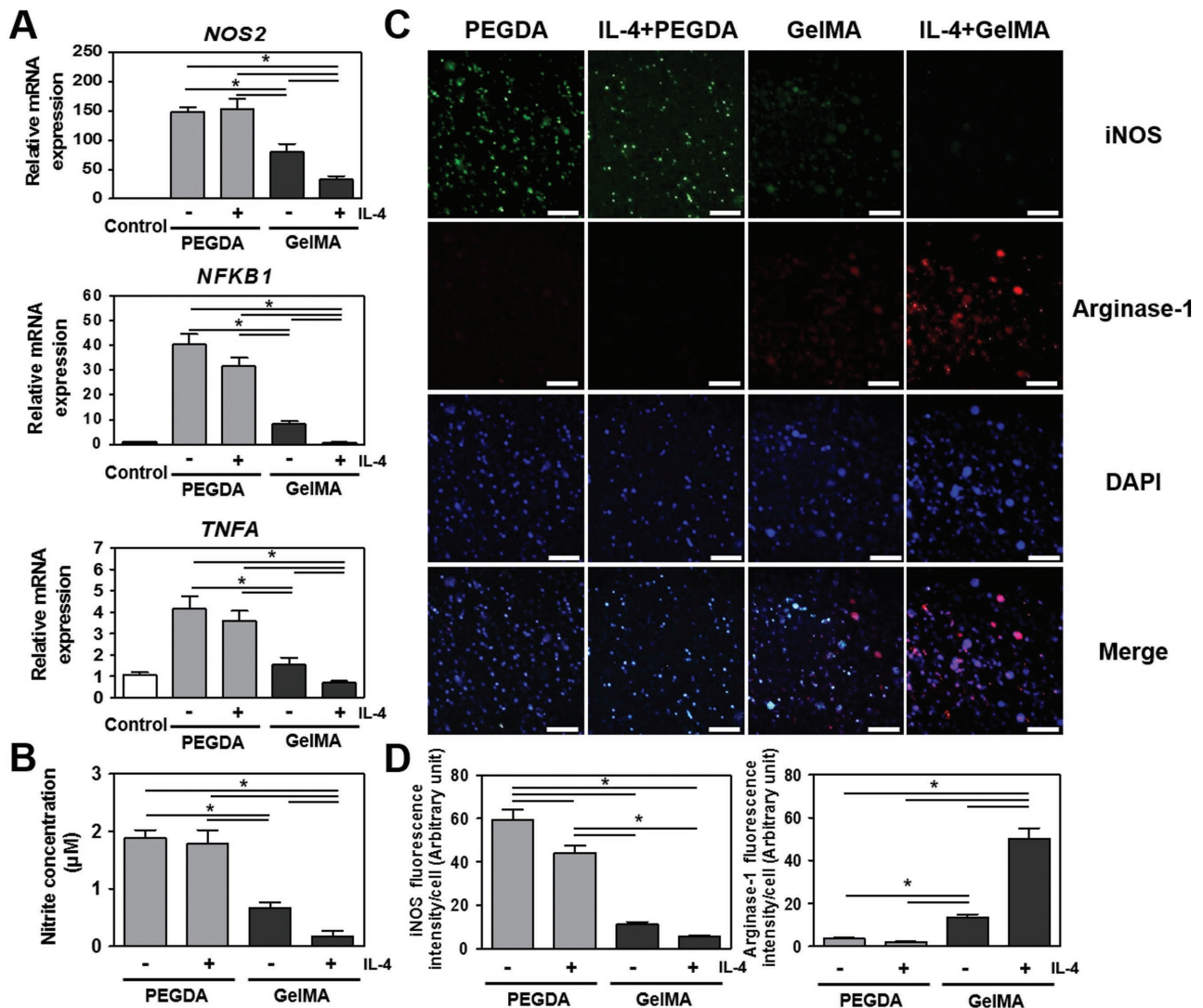


**Figure 2.** In vitro immune response of human monocytic THP-1 cells encapsulated in PEGDA and GelMA hydrogels in the absence or presence of IL-4 for 6 d. A) Real-time PCR of inflammatory genes. B) Biochemical quantification of nitrite production. C) Images of THP-1 cells fluorescently stained for M1-related iNOS, M2-related Arginase-1 and DAPI. D) Quantitative analysis of images. Scale bar represents 100 μm. The data are shown as the mean ± SEM (\*,  $p < 0.05$ ).

control group. Nevertheless, IL-4 stimulation decreased the levels of all markers even further in GelMA hydrogels. However, the expression levels of *NOS2*, *NFKB1*, *TNFA*, and nitrite from THP-1 cells in PEGDA hydrogels remained largely unaffected after exposure of THP-1 cells to IL-4. In line with these observations, immunohistochemistry revealed that cells encapsulated in PEGDA hydrogels demonstrated intense positive staining for M1 marker iNOS<sup>[28d,31]</sup> and negative for M2 marker Arginase-1,<sup>[28d,32]</sup> whereas THP-1 cells in GelMA demonstrated the exact opposite staining pattern (Figure 2C,D). In addition, both PEGDA and GelMA hydrogels appeared to generate pro-inflammatory responses even in the absence of polarizing stimuli, with PEGDA having a stronger effect. Although the expression and role of iNOS and Arginase-1 are better defined in mouse models, recent work has also reported their expression and function in human macrophages.<sup>[31,33]</sup>

Our results demonstrate the potency of cell–biomaterial interactions to program monocytes into a specific polarized macrophage phenotype. Paradoxically, the data also suggest that bioinert materials such as PEGDA hydrogels can elicit a proinflammatory immune response.<sup>[29]</sup> However, these pro-inflammatory responses induced in GelMA in the absence of IL-4 stimulation would not be able to explain the mechanism, clearly. Moreover, biomaterial composition can even prevent monocytes from responding to cytokines such as IL-4 that would drive implant integration and tissue regeneration. The mechanism by which biomaterials can drive monocytes into such distinct macrophage phenotypes has remained largely unknown. However, we reasoned that our approach of simultaneously using two comparable (e.g., in terms of their mechanical properties and IL-4 release profiles) yet distinct hydrogel systems might yield valuable information

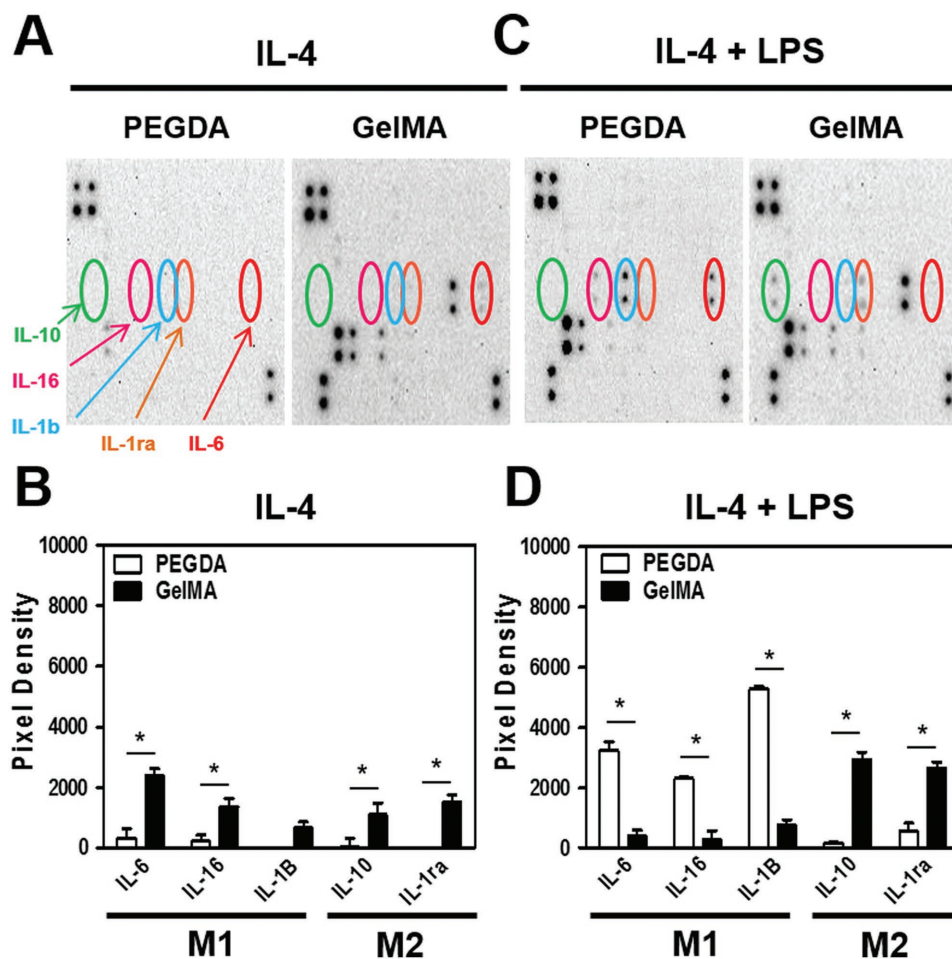


**Figure 3.** Pro- and anti-inflammatory cytokine release of human monocytic THP-1 cells in IL-4 incorporated PEGDA and GelMA hydrogels for 6 d. A,C) Cytokine release assay and its B,D) quantitative analysis of THP-1 cells exposed to both M1 inducing lipopolysaccharides (LPS) and M2 macrophage inducing IL-4 in PEGDA and GelMA hydrogels. The data are shown as the mean  $\pm$  SEM (\*,  $p < 0.05$ ).

on how biomaterials composition can control macrophage polarization.

#### 2.4. Hydrogel Composition Determines Macrophage Cytokine Release Profile

To confirm the M1 and M2 fingerprints, we additionally visualized and semiquantified the M1–M2 macrophage specific cytokine release profiles from human monocytic THP-1 cells encapsulated in either PEGDA or GelMA hydrogels in the presence of IL-4. In particular, the secretion of proinflammatory cytokines IL-1B, IL-6, and IL-16 as well as the anti-inflammatory cytokines interleukin-1 receptor antagonist (IL-1RA) and IL-10 were investigated (Figure 3A,B). THP-1 cells encapsulated in GelMA demonstrated significantly higher levels of all tested anti-inflammatory cytokines as compared to those encapsulated in PEGDA. Interestingly, no LPS stimulated THP-1 cells encapsulated in GelMA also demonstrated a modest trend of higher expression levels of proinflammatory cytokines as compared to the M1 inducing PEGDA.

It is of note that these experiments were performed in the presence of M2 inducing IL-4, but in the absence of an M1

inducing factor. However, wound and implant sites naturally contain a combination of stimuli that favor both M1 and M2 polarization at different stages of healing. We therefore encapsulated THP-1 cells in PEGDA or GelMA hydrogels and exposed them to both LPS and IL-4, which drove the THP-1 cells to M1 and M2 polarization, respectively. Remarkably, under these more biologically complex conditions, we observed that THP-1 cells in PEGDA hydrogels expressed significantly higher levels of all M1-related cytokines, whereas those in GelMA hydrogels expressed significantly higher levels of all M2-related cytokines (Figure 3C,D). In accordance with previous studies, although in 2D culture, the secretion of the proinflammatory molecules IL-1 $\beta$  and TNF- $\alpha$  increased dramatically following human primary monocyte interactions with PEG-only hydrogel films as compared with tissue culture polystyrene.<sup>[34]</sup> In fact, supplementation of the M1 inducing LPS to THP-1 cells in GelMA hydrogels further increased the expression levels of M2-related cytokines while decreasing those of M1-related cytokines, as compared to IL-4 alone. In essence, these results demonstrated that LPS stimulation did not reverse the M2 polarization of macrophages in GelMA in the presence of IL-4 and unexpectedly enhanced the polarization.

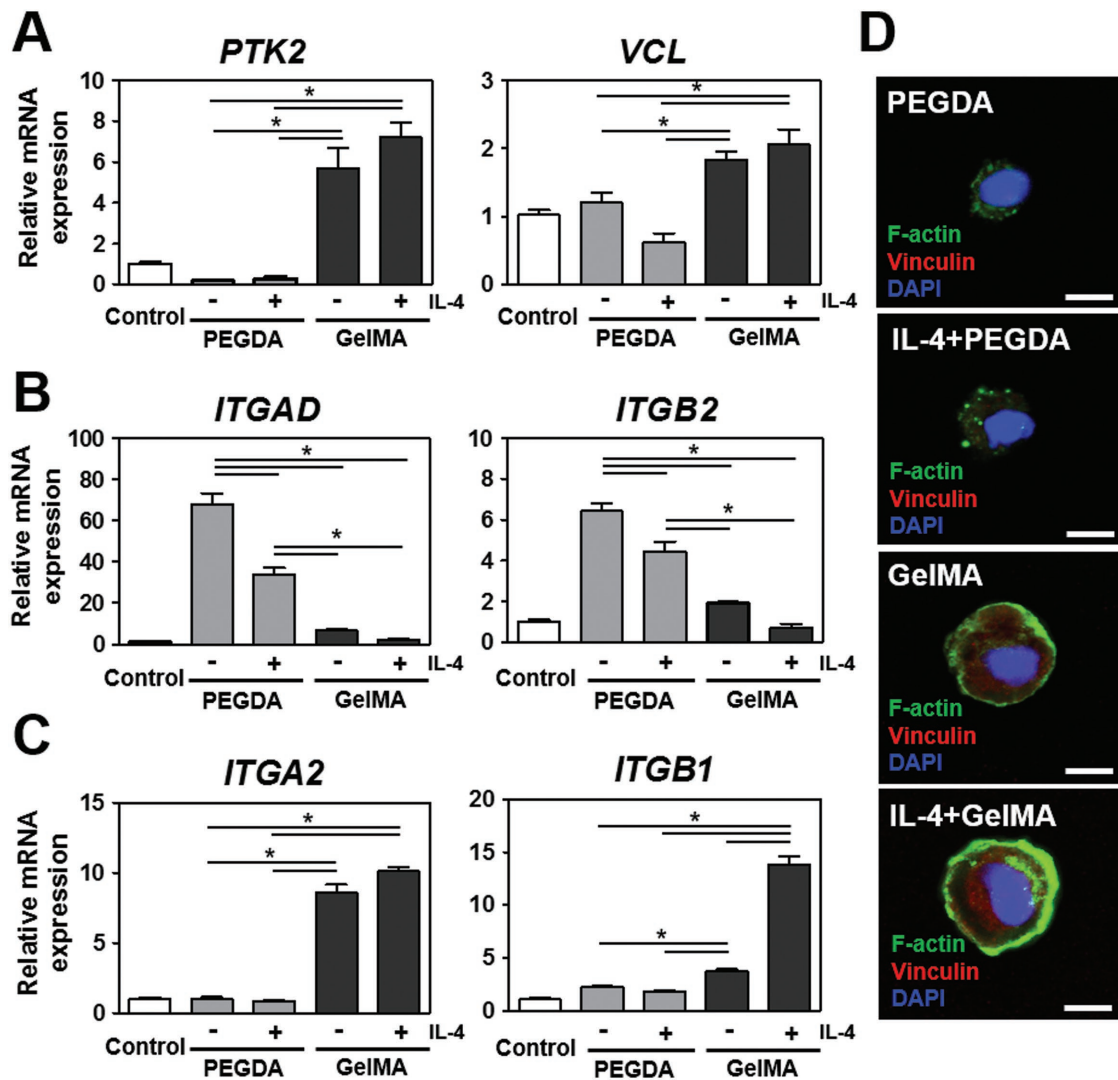


**Figure 4.** Changes in cytoskeletal organization and focal adhesion molecules in IL-4 cytokine incorporated PEGDA and GelMA hydrogels for 6 d. A) Real-time PCR of protein tyrosine kinase 2 (*PTK2*) and vinculin (*VCL*). B) Real-time PCR of monocyte-related integrin receptors (Integrin  $\alpha$ D (*ITGAD*) and Integrin  $\beta$ 2 (*ITGB2*)). C) Real-time PCR of collagen matrix-related integrin receptors (Integrin  $\alpha$ 2 (*ITGA2*) and Integrin  $\beta$ 1 (*ITGB1*)). D) Images of F-actin and vinculin of THP-1 cells encapsulated in IL-4 cytokine incorporated PEGDA and GelMA hydrogels. Scale bar represents 10  $\mu$ m. The data are shown as the mean  $\pm$  SEM (\*,  $p < 0.05$ ).

### 2.5. Hydrogel Composition Affects the THP-1 Cells' Integrin Expression and Cytoskeletal Organization

A key difference between the hydrogels used in this study is the presence or absence of cell–adhesive motifs. Specifically, GelMA hydrogels contain cell–adhesive sequences while PEGDA hydrogels do not. We therefore hypothesized that the difference in macrophage phenotype between the two hydrogel systems might be regulated through attachment and downstream signaling, which is mediated via integrin subunits and focal adhesions. To this end, we determined the relative gene expression levels of focal adhesion kinase (*PTK2*), vinculin (*VCL*), monocyte-related integrin receptors Integrin  $\alpha$ D (*ITGAD*) and  $\beta$ 2 (*ITGB2*), and collagen matrix-related integrin receptors integrin  $\alpha$ 2 (*ITGA2*) and  $\beta$ 1 (*ITGB1*) in cells encapsulated in PEGDA and GelMA hydrogels with or without IL-4. PEGDA

hydrogel's inability to provide binding sites was mirrored by the strong decrease in *PTK2* expression levels compared to GelMA hydrogels and tissue culture plastic grown control samples. By contrast, GelMA hydrogels induced an increase in monocyte expression of *PTK2* and *VCL* (Figure 4A). Low levels of integrin  $\alpha$ D and  $\beta$ 2—alternatively known as CD11d and CD18—are correlated with monocyte migration, whereas high levels of these integrins are associated with proinflammatory macrophages.<sup>[35]</sup> In line with this, monocytes encapsulated in PEGDA hydrogels showed significantly high levels of *ITGAD* and *ITGB2* expression, whereas the expression level of these integrin proteins were found to be low when encapsulated in GelMA hydrogels (Figure 4B). Such an increase in upregulation of integrin  $\alpha$ D $\beta$ 2 in monocytes/macrophages might be due to the stimulation of proinflammatory responses resulting from the IL-4 presence with lesser effects arising from the absence of available binding

sites in PEGDA hydrogels. Migration and collagen attachment is mediated via integrins such as  $\alpha 2$  and  $\beta 1$ , which are also known as CD49b and CD29.<sup>[36]</sup> The expression of *ITGA2* and *ITGB1* was drastically upregulated in GelMA hydrogels but remained unchanged in PEGDA hydrogels (Figure 4C). These results demonstrated that the composition of the biomaterial effectively determines human monocytic THP-1 cells' expression of adhesion molecules. In addition to facilitating cell attachment, integrins also play an important and versatile role in multiple signaling pathways. Therefore, biomaterials can program the cellular response to a given microenvironment, which includes their response to macrophage polarizing cytokines.

To investigate whether the changes in integrin expression translated to cytoskeletal changes, we investigated the expression and distribution of vinculin and F-actin using immunocytochemistry. Vinculin is involved in the linkage of integrin adhesion molecules to the actin cytoskeleton. Therefore, vinculin and F-actin are both sensitive and responsive to biological and mechanical stimuli mediated via integrin-based cell attachment.<sup>[37]</sup> THP-1 cells encapsulated in GelMA hydrogels showed intense staining for vinculin, whereas the staining of those encapsulated in PEGDA hydrogels were consistently below the detection limit (Figure 4D). The latter result might be explained by the diminished biomechanical stimulation due to the lack of cell binding sites in PEGDA hydrogels. Furthermore, THP-1 cells in PEGDA hydrogels demonstrated clump-like cytoplasmic aggregates of F-actin, which has been reported to correlate with monocyte-to-macrophage transition as well as the migration and function of various immune cells.<sup>[38]</sup> F-actin staining of THP-1 cells in GelMA hydrogels revealed the presence of a prominent cortical shell, which has been reported to be indicative of M2 commitment.<sup>[39]</sup> Together, these results demonstrated that biomaterial-induced changes in integrin expression effectively translated to or tightly correlated with marked changes in cell behavior and cytoskeletal organization.

## 2.6. Integrin $\alpha 2\beta 1$ -Mediated Binding of THP-1 Cells to Biomaterials is Required for M2 Macrophage Polarization

Based on the significant changes in integrin expression and subsequent cytoskeletal reorganization, we hypothesized that integrins might potentially affect downstream signaling pathways and thereby control macrophage polarity. To this end, THP-1 cells encapsulated in GelMA hydrogels were exposed to a neutralizing antibody for integrin  $\alpha 2\beta 1$  in the presence or absence of the M2 inducing cytokine IL-4. Similar to our previous experiments, THP-1 cells in GelMA hydrogels expressed high levels of M1-related CD86 and low levels of M2-related CD206, and IL-4 supplementation further decreased CD86 to undetectable levels and significantly increased CD206 expression. Remarkably, blocking integrin  $\alpha 2\beta 1$  strongly increased CD86 expression and reduced CD206 expression below the detection limit, even in the presence of IL-4 (Figure 5A,B). THP-1 cells encapsulated in GelMA hydrogels that were exposed to integrin  $\alpha 2\beta 1$  blocker therefore mirrored the behavior of human monocytic THP-1 cells encapsulated in PEGDA. Addition of noninhibitory isotype control antibody was undistinguishable

from the untreated control group. This suggested that the integrin  $\alpha 2\beta 1$  induced polarization through its integrin  $\alpha 2\beta 1$  binding domain rather than its conserved antibody domain. Furthermore, immunohistochemical staining revealed that blocking integrin  $\alpha 2\beta 1$  lowered the expression of F-actin and vinculin while reducing the cell size therefore more closely resembling THP-1 cells encapsulated in PEGDA hydrogels. These results suggested the effective blocking of integrin  $\alpha 2\beta 1$ -mediated binding and thus limiting cell–biomaterial interactions (Figure 5C). Moreover, this blockage mitigated the high levels of cytoskeletal-related *PTK2* and *VCL* expression in GelMA hydrogels, strongly increased expression of M1-related *IRF5* and *IL6*, and decreased expression of M2-related *STAT6* and *IL10* (Figure 5D). In summary, integrin  $\alpha 2\beta 1$  appeared to play a pivotal role in macrophage polarization (Figure 5E). In particular, IL-4 incorporated GelMA hydrogel biomaterials were observed to drive monocytes into the M2 macrophage phenotype through integrin  $\alpha 2\beta 1$  attachment, most likely via *STAT6* activation. The inability of monocytes to attach to biomaterials via integrin  $\alpha 2\beta 1$ —either through pharmacological blockage or absence of available binding sites—results in the generation of M1 macrophages, most likely through *IRF5* activation. This might also suggest that M1 is potentially a default phenotype.

To confirm that the observation of integrin  $\alpha 2\beta 1$ -mediated macrophage polarization was not restricted to the THP-1 monocytic cell line, we also seeded human primary monocytes on plates coated with integrin  $\alpha 2\beta 1$  peptide (the type I collagen  $\alpha 1(I)$ -CB3 fragment Asp–Gly–Glu–Ala or DGEA) and investigated their polarization status after 6 d (Figure S8A,B, Supporting Information). The cells cultured on DGEA-coated plates expressed higher levels of the M2 marker CD206, with no noticeable changes in the level of M1 marker expressions (in this case calprotectin),<sup>[5]</sup> compared to bovine serum albumin (BSA) control group (Figure S8A, Supporting Information) indicating a shift toward M2 phenotype in cells cultured on DGEA-coated surfaces. Notably, cells cultured on DGEA-coated plates also demonstrated significantly higher levels of the anti-inflammatory cytokine, IL-10, compared to the BSA control groups (Figure S8B, Supporting Information) which again is an indication of a shift toward an M2 phenotype.<sup>[40]</sup> This data also showed an increase in IL-6 production by cells on the DGEA-coated plates. While IL-6 is typically considered a proinflammatory cytokine, recent *in vivo* data have clearly shown that it also enhances the polarization of alternatively activated macrophages (i.e., M2 phenotype).<sup>[41]</sup> Collectively, these data indicate that simple DGEA motives (which is recognized by integrin  $\alpha 2\beta 1$ ) induced a partial shift of human primary monocytes toward the M2 macrophage phenotype and created a cytokine environment that promoted M2 macrophages polarization, even in a 2D culture environment.<sup>[41]</sup>

By extension, this conclusion stipulates that PEG-based hydrogels are bioinert<sup>[42]</sup> and do not present integrin binding sites and are prone to cause M1 macrophage polarization. Further studies with other bioinert polymers can elucidate whether this conclusion can be generalized. Several such bioinert biomaterials are often viewed as immunoprotective or immune-shielding. However, the inability of these materials to interact with immune cells (e.g., macrophages) in a direct manner can potentially drive the immune response in a

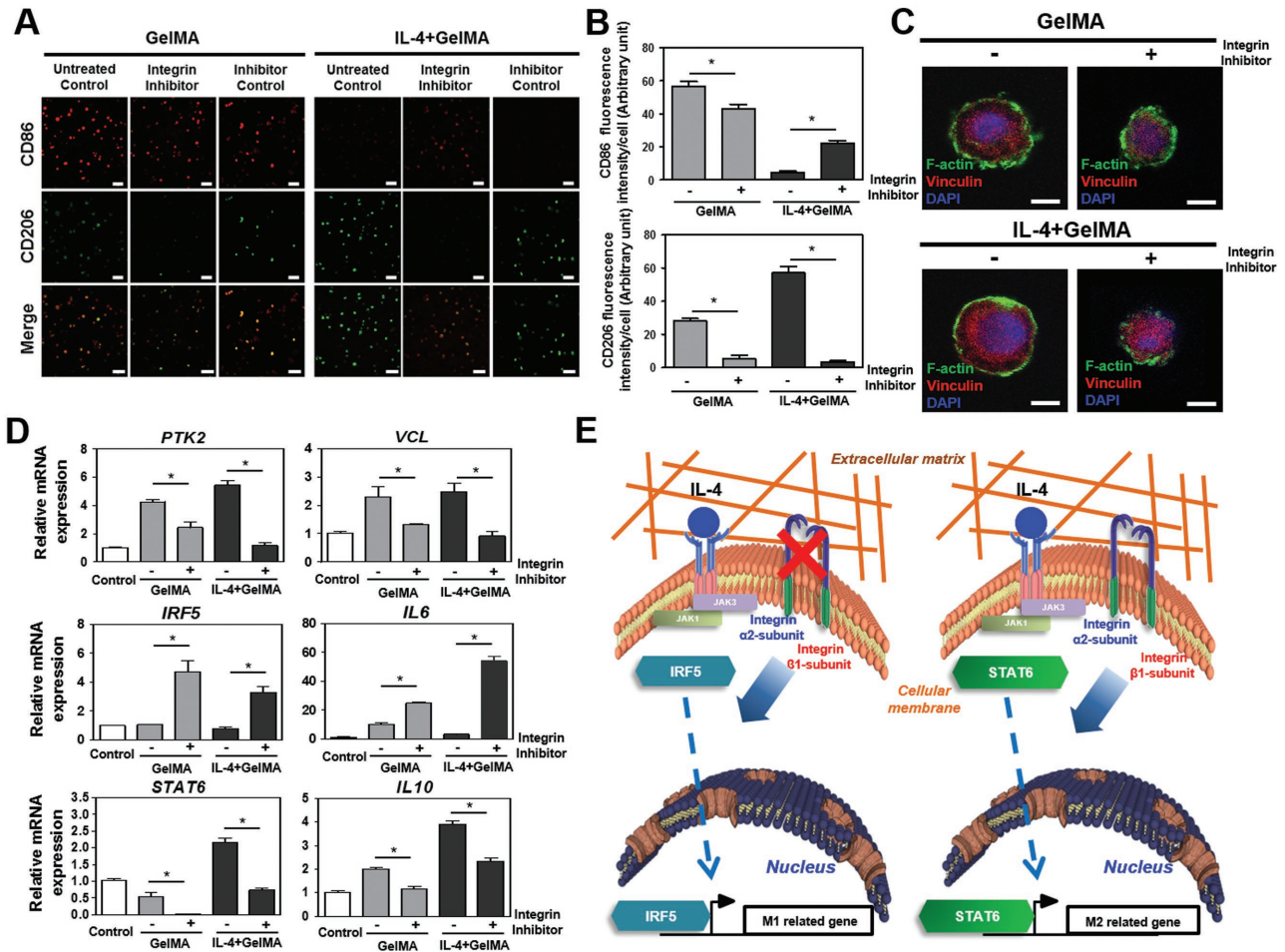


**Figure 5.** The effect of integrin  $\alpha 2 \beta 1$  inhibition on macrophage polarity in IL-4 cytokine incorporated GelMA hydrogel. A) Confocal images of M1 and M2 macrophage surface markers CD86 and CD206 with or without integrin  $\alpha 2 \beta 1$  receptor inhibitor or noninhibitory isotype control antibody. Scale bar represents 100  $\mu$ m. B) Quantitative analysis of images. C) Confocal images of focal adhesion molecule expression with or without integrin  $\alpha 2 \beta 1$  receptor inhibitor. Scale bar represents 10  $\mu$ m. D) mRNA expression levels of M1 and M2 macrophage markers and focal adhesion molecules in IL-4 incorporated GelMA hydrogel with or without integrin  $\alpha 2 \beta 1$  receptor inhibitor. E) Proposed mechanism via which biomaterials are able to prime human monocytic THP-1 cells into either an M1 or M2 macrophage phenotype. The data are shown as the mean  $\pm$  SEM (\*,  $p < 0.05$ ).

deleterious direction. Indeed, these materials are more prone to deleterious immune responses and result in relatively intense fibrous capsule formation upon implantation. This foreign body response is at least in part generated via M1 macrophages, which as reported in this work are generated when monocytes are unable to interact with the implant via integrins. Although the concept that the absence of a cell–biomaterial interaction can potently determine cell fates is novel, there is a well-established precedence within the domain of cell–cell interactions. In particular, our observations are reminiscent of the immunological failsafe that safeguards major histocompatibility complex (MHC) function. In this system, the immune system triggers programmed cell death of cells that present unfavorable antigens via their MHC.<sup>[43]</sup> Intuitively, it might therefore be expected that the absence of MHC expression might provide a degree of immunoprotection.<sup>[44]</sup> However, the immune system also triggers programmed cell death in cells that do not allow this interaction. Similarly, the immune system might attempt to destroy or isolate (via fibrous capsule formation) implants.

In our study, we revealed that biomaterials designed to evade the immune system recognition by not presenting any integrin recognition motifs induce a proinflammatory M1 macrophage phenotype. It might therefore be reasoned that our immune system has evolved multiple distinct safeguards, which by default elicit a deleterious immune response when unable to interact with its target, be it a cell or biomaterial. In other words, the presence of encapsulated macrophages, acquiring an M2 phenotype, in vivo can trigger a faster observation of the initial inflammation by facilitating the conversion of M1 macrophages to M2 macrophages. However, the complex nature of the implant microenvironment in vivo and the presence of other immune cells (such as T-cells) must be also taken into account and the means for long term cytokine induction (via controlled delivery systems) must be considered for potent in vivo effects.

As such, biomaterial-based implants can be made truly immune-compatible by including motifs that prime the immune system to drive integration rather than rejection.

Incorporating cell attachment sites into the design of biomaterials will thus not only stimulate the encapsulated therapeutic cells, but also steer the host's immune system toward a healing response. However, the amount of the inflammation must also be controlled; otherwise long-term presence of M2 macrophages can result in fibrosis.<sup>[45]</sup> Indeed, recent studies have indicated that this approach is both feasible and practical; coating bioinert biomaterials with decellularized ECM decreased M1 macrophage induction and the subsequent chronic inflammatory response.<sup>[46]</sup> Although our data indicated that integrin  $\alpha 2\beta 1$  played an essential role in M2 macrophage induction, other integrins could potentially affect macrophage proliferation distinctly as they interact with different ligands.<sup>[47]</sup> Indeed, decorating biomaterials with the integrin binding tripeptide Arg–Gly–Asp has been reported to induce fibrosis.<sup>[17b,18c]</sup> Systematic analysis of the effects of integrins, and other adhesive moieties, on macrophage polarity could resolve such contradictions and provide design principles on how to create next-generation biomaterials that controllably induce M1 or M2 macrophage polarization.

In summary, incorporating cell binding domains into biomaterials to facilitate integrin interactions in 3D microenvironment, such as those with  $\alpha 2\beta 1$ , to steer the host's immune system toward a natural healing response represents an exciting and novel opportunity to control and improve the clinical outcomes of biomaterial-based implants and cell therapies.

### 3. Conclusion

Biomaterial-mediated immunomodulation by programming macrophage polarity is a promising tool in tissue engineering, regenerative medicine, and implantology to decrease adverse immune reactions, accelerate implant integration, facilitate tissue regeneration, and increase implant lifetime. Here, we present a mechanism and 3D biomaterial-based approach for immunomodulation, which controls the balance between inducing proinflammatory M1 macrophages and regenerative M2 macrophages. We have shown the ability of 3D encapsulated human monocytic THP-1 cells to interact with IL-4 stimulation and that the biomaterials through integrin  $\alpha 2\beta 1$  has a direct effect on macrophage phenotype by inducing M2 macrophages, whereas blocking this mechanism induces M1 macrophages. We have thereby further uncovered the essential and pivotal role of integrins in the immune response. Overall, biomaterial-based control over macrophages represents a novel technique to obtain a fundamental understanding of macrophage behavior and is a strong therapeutic tool for immunomodulation for implants, drug, and cell delivery systems.

### 4. Experimental Section

**Biomaterials:** PEGDA, gelatin (Type A, 300 bloom from porcine skin), and methacrylic anhydride were purchased from Sigma-Aldrich (Wisconsin, USA). GelMA was synthesized as described previously.<sup>[48]</sup> Hydrogels were crosslinked using an UV source (Omnicure S2000, Ontario, Canada).

**Fabrication of Hydrogel Constructs:** Freeze dried prepolymer solutions were mixed in Dulbecco's Phosphate Buffered Saline (DPBS) with

2-hydroxy-1-(4-(hydroxyethoxy)phenyl)-2-methyl-1-propanone (Irgacure 2959, CIBA Chemicals) and placed at 80 °C until fully dissolved. Recombinant human IL-4 (R&D Systems) was added when desired at a final concentration of 10 ng mL<sup>-1</sup>. Human monocytic THP-1 cells were encapsulated in the prepolymer at a final concentration of 6 × 10<sup>6</sup> cells per mL. Prepolymer samples were divided in 20 μL samples and photocrosslinked using 800 mW cm<sup>-2</sup> UV light (Omnicure S2000, EXFO Photonic Solutions Inc.) for 10 or 40 s for GelMA and PEGDA hydrogels, respectively. Constructs were cultured in Dulbecco's Modified Eagle Medium (Gibco BRL) supplemented with 10% (v/v) fetal bovine serum (FBS) (Gibco BRL) and 100 units per mL penicillin (Gibco BRL) in an incubator with 5% (v/v) CO<sub>2</sub> at 37 °C. Medium was refreshed every 2 d.

**Compressive Modulus:** 200 μL was formed and allowed to incubate at 37 °C in DPBS for 24 h. Hydrogels were tested at a rate of 20% strain per min on an Instron 5542 mechanical tester. The compressive modulus was determined as the slope of the linear region corresponding with 0–5% strain.

**IL-4 Release Kinetics:** Hydrogels were submerged in 200 μL DPBS and incubated at 37 °C without agitation for up to 7 d. At predetermined time points, the supernatant was retrieved and replaced with fresh buffer. The IL-4 concentration in the supernatant was quantified using a human IL-4 ELISA Kit (Quantikine ELISA, R&D Systems).

**Viability and Proliferation of Human Monocytic THP-1 Cells:** 24 h postencapsulation, live and dead cells were visualized using calcein-AM and ethidium homodimer (Invitrogen), photographed using an inverted fluorescence microscope (Nikon TE 2000-U), and quantified using National Institutes of Health (NIH) ImageJ software. Cell proliferation was measured up to 7 d of culture using Alamar Blue assay (Invitrogen).

**Hydrogel Swelling Analysis:** Polymerization was performed as described above in "Fabrication of Hydrogel Constructs." Immediately following the hydrogel formation, disks (8 mm in radius) of each composition were punched from a flat thin sheet and placed in DPBS at 37 °C for 24 h. Disks were removed from DPBS and blotted with a KimWipe to remove the residual liquid and the swollen weight was recorded. Samples were then lyophilized and weighed once more to determine the dry weight of the polymer. The mass swelling ratio was then calculated as the ratio of swollen hydrogel mass to the mass of dry polymer.

**Immunohistochemical Staining:** Samples were fixed in 4% (v/v) formalin and permeabilized with 0.1% (v/v) Triton X-100 for 30 min. Molecules of interest were labeled using a primary antibody such as Anti-CD86 antibody (Abcam), anti-calprotectin antibody (Thermo Scientific), antimannose receptor antibody (CD206, Abcam), antivinculin antibody (Sigma), anti-NOS2 antibody (Santa Cruz Biotechnology), and anti-Arginase-1 antibody (Santa Cruz Biotechnology). Target molecules were then visualized using Alexa 488 or Alexa 594 conjugated secondary antibodies (Molecular Probes). F-Actin was visualized using rhodamine–phalloidin (Invitrogen). Samples were counterstained with 4,6-diamidino-2-phenylindole (DAPI, Vector Laboratories Inc.) and photographed using either a fluorescence microscope (IX71 inverted microscope, Olympus) or an inverted laser scanning confocal microscope (SP5 X MP, Leica Microsystems). Signal intensities of CD86, CD206, iNOS, and arginase-1 of individual cells were quantitatively analyzed using NIH ImageJ software.

**Quantitative Real-Time Polymerase Chain Reaction (PCR):** Total RNA was extracted using TRIzol (Invitrogen), quantified using a Nanodrop2000 (Thermo Fisher Scientific), and synthesized into cDNA synthesis using SuperScript III First-Strand Synthesis SuperMix (Invitrogen). For quantitative real-time PCR analysis, 20 ng of input RNA was amplified in an IQ5 detection system (Biorad) using SYBR Green Master Mix (Bio-Rad) and 500 nmol L<sup>-1</sup> of gene-specific primers. All mRNA expression levels were normalized to glyceraldehyde-3-phosphate dehydrogenase. Primer sequences are listed in Table S1 of the Supporting Information.

**Cytokine Expression Profiling:** Hydrogels embedded THP-1 cells were cultured for 6 d after which fresh medium was allowed to be conditioned for 24 h and laden onto a human cytokine antibody array

(Human Cytokine Array C6, RayBiotech Inc), processed, and detected according to manufacturer's protocol. Invariant set normalization was used to normalize the interarray intensity (Image pro PLUS, Media Cybernetics Inc.).

**Integrin Receptor Blocking:** Human monocytic THP-1 cells were pretreated with 10  $\mu\text{g mL}^{-1}$  Anti-Integrin alpha 2+beta 1 antibody (Abcam) or noninhibitory isotype control antibody (Abcam) for 30 min at 37 °C, washed, encapsulated in GelMA hydrogels containing IL-4, and cultured for 6 d.

**Nitrite Production:** After 6 d of culture, 50  $\mu\text{L}$  of supernatant was retrieved and processed according to the manufacturer's protocols (Griess reagent, Promega). The absorbance of the developed solution was measured at a wavelength of 550 nm using an ELISA Microplate Reader (VersaMax, Molecular Device).

**Fabrication of  $\alpha 2\beta 1$  Integrin Ligand Peptide Asp-Gly-Glu-Ala (DGEA)-Coated Substrate:** To prepare the DGEA-coated coverslips, acid-etched glass coverslips were incubated with 0.1  $\text{mg mL}^{-1}$  MAPTriX-C-DGEA peptide (Amsbio) or BSA (used as a negative control) in  $500 \times 10^{-3}$  M  $\text{NaHCO}_3$  solution for 1 h at room temperature. Coverslips were washed with DPBS and used immediately. Buffy coat samples were obtained from healthy volunteers in accordance with the relevant guidelines after obtaining informed written consent and approval of local ethics committee (all approved by the National Blood Service, UK). Human peripheral blood mononuclear cells (PBMCs) were obtained from heparinized blood by Histopaque-1077 density gradient centrifugation. Monocytes were isolated from PBMCs using the Miltenyi Biotec magnetic cell separation system (positive selection with CD14 MicroBeads and LS columns) as per the manufacturer's instructions. This method yielded 95% pure monocytes as determined by flow cytometric analysis of CD14 expression. Purified monocytes were cultured at  $5 \times 10^5$  cells per coverslip in RPMI-1640 supplemented with 10% FBS, 100 U  $\text{mL}^{-1}$  penicillin, 100  $\mu\text{g mL}^{-1}$  streptomycin (referred to henceforth as "RPMI complete medium"), and 10  $\text{ng mL}^{-1}$  macrophage-colony stimulating factor (M-CSF) (Miltenyi Biotec) in 24-well tissue culture-treated plates. Included controls were: M1 (50  $\text{ng mL}^{-1}$  granulocyte-macrophage-CSF (Miltenyi Biotec) + 20  $\text{ng mL}^{-1}$  IFN- $\gamma$  (R&D Systems)), M2 (50  $\text{ng mL}^{-1}$  M-CSF + 20  $\text{ng mL}^{-1}$  IL-4 (Miltenyi Biotec)), and M-CSF (10  $\text{ng mL}^{-1}$  M-CSF). Samples were incubated at 37 °C, 5%  $\text{CO}_2$  for 6 d, with fresh complete medium containing cytokines added on Day 3. On Day 6, samples were stained with 1  $\mu\text{g mL}^{-1}$  rabbit antihuman mannose receptor antibody (Abcam) and 2  $\mu\text{g mL}^{-1}$  mouse antihuman calprotectin antibody (Thermo Scientific) (M2 and M1 markers, respectively)<sup>[5]</sup> diluted in 5% goat serum in PBS. Secondary antibody staining was then carried out using 8  $\mu\text{g mL}^{-1}$  each of goat antirabbit Alexa Fluor 488-conjugated antibody and goat antimouse Rhodamine Red-X-conjugated antibody (both from Thermo Fisher Scientific). Finally, samples were counterstained with 250  $\text{ng mL}^{-1}$  DAPI and mounted on microscope slides. Images were captured using an IMSTAR automated fluorescence microscope. Image analysis and quantification was carried out using CellProfiler software v 2.1.1. Furthermore, supernatants were collected and assayed for the cytokines IL-6 and IL-10 using ELISA DuoSet kits (R&D Systems) as per the manufacturer's instructions.

**Statistical Analysis:** At least three independent sets of experiments for each condition were performed in triplicate. Data were pooled and statistically expressed as mean  $\pm$  standard error of mean. Two-way analysis of variance was used for analysis of quantitative values, and Tukey's posthoc test was used for all pair-wise comparisons among groups. Differences were considered significant at  $p < 0.05$  and were indicated with an asterisk. The SPSS software package (version 12.0; SPSS Inc.) was used to perform statistical tests.

## Supporting Information

Supporting Information is available from the Wiley Online Library or from the author.

## Acknowledgements

B.-H.C. and S.R.S. contributed equally to this work. The authors acknowledge funding from the National Science Foundation (EFRI-1240443), UK Engineering and Physical Sciences Research Council (EP/N006615/1), EU FP 7 IMMODGEL (602694), and the National Institutes of Health (EB012597, AR057837, DE021468, HL099073, and R56AI105024). B.-H.C. was supported by Basic Science Research Program through the National Research Foundation of Korea (NRF) funded by the Ministry of Education, Science and Technology (NRF-2016R1D1A1B03934876). J.L. acknowledges financial support from Innovative Research Incentives Scheme Veni #14328 of the Netherlands Organization for Scientific Research (NWO).

## Conflict of Interest

The authors declare no conflict of interest.

## Keywords

hydrogels, immune modulation, integrin, M1, M2, macrophage polarization

Received: March 6, 2017

Revised: June 17, 2017

Published online: August 7, 2017

- [1] a) C. Gretzer, L. Emanuelsson, E. Liljensten, P. Thomsen, *J. Biomater. Sci., Polym. Ed.* **2006**, *17*, 669; b) D. T. Luttkhuizen, M. C. Harmsen, M. J. Van Luyn, *Tissue Eng.* **2006**, *12*, 1955.
- [2] a) J. M. Anderson, A. Rodriguez, D. T. Chang, *Semin. Immunol.* **2008**, *20*, 86; b) G. Broughton 2nd, J. E. Janis, C. E. Attinger, *Plast. Reconstr. Surg.* **2006**, *117*, 12S.
- [3] a) F. Porcheray, S. Viaud, A. C. Rimaniol, C. Leone, B. Samah, N. Dereuddre-Bosquet, D. Dormont, G. Gras, *Clin. Exp. Immunol.* **2005**, *142*, 481; b) A. Mantovani, A. Sica, S. Sozzani, P. Allavena, A. Vecchi, M. Locati, *Trends Immunol.* **2004**, *25*, 677.
- [4] V. P. Yakubenko, A. Bhattacharjee, E. Pluskota, M. K. Cathcart, *Circ. Res.* **2011**, *108*, 544.
- [5] H. M. Rostam, S. Singh, F. Salazar, P. Magennis, A. Hook, T. Singh, N. E. Vrana, M. R. Alexander, A. M. Ghaemmaghami, *Immunobiology* **2016**, *221*, 1237.
- [6] J. M. Anderson, A. Rodriguez, D. T. Chang, *Semin. Immunol.* **2008**, *20*, 86.
- [7] W. G. Brodbeck, J. Patel, G. Voskerician, E. Christenson, M. S. Shive, Y. Nakayama, T. Matsuda, N. P. Ziats, J. M. Anderson, *Proc. Natl. Acad. Sci. USA* **2002**, *99*, 10287.
- [8] B. N. Brown, S. F. Badylak, *Acta Biomater.* **2013**, *9*, 4948.
- [9] A. Moshaverinia, C. Chen, X. Xu, S. Ansari, H. H. Zadeh, S. R. Schriker, M. L. Paine, J. Moradian-Oldak, A. Khademhosseini, M. L. Snead, S. Shi, *Adv. Funct. Mater.* **2015**, *25*, 2296.
- [10] a) M. L. Pinto, E. Rios, A. C. Silva, S. C. Neves, H. R. Caires, A. T. Pinto, C. Duraes, F. A. Carvalho, A. P. Cardoso, N. C. Santos, C. C. Barrias, D. S. Nascimento, O. P. Pinto-do, M. A. Barbosa, F. Carneiro, M. J. Oliveira, *Biomaterials* **2017**, *124*, 211; b) J. Jiang, Z. Li, H. Wang, Y. Wang, M. A. Carlson, M. J. Teusink, M. R. MacEwan, L. Gu, J. Xie, *Adv. Healthcare Mater.* **2016**, *5*, 2993; c) S. Minardi, B. Corradetti, F. Taraballi, J. H. Byun, F. Cabrera, X. Liu, M. Ferrari, B. K. Weiner, E. Tasciotti, *Ann. Biomed. Eng.* **2016**, *44*, 2008.

- [11] H. M. Rostam, S. Singh, N. E. Vrana, M. R. Alexander, A. M. Ghaemmaghami, *Biomater. Sci.* **2015**, *3*, 424.
- [12] L. R. Madden, D. J. Mortisen, E. M. Sussman, S. K. Dupras, J. A. Fugate, J. L. Cuy, K. D. Hauch, M. A. Laflamme, C. E. Murry, B. D. Ratner, *Proc. Natl. Acad. Sci. USA* **2010**, *107*, 15211.
- [13] V. W. Wong, K. C. Rustad, S. Akaishi, M. Sorkin, J. P. Glotzbach, M. Januszzyk, E. R. Nelson, K. Levi, J. Paterno, I. N. Vial, A. A. Kuang, M. T. Longaker, G. C. Gurtner, *Nat. Med.* **2012**, *18*, 148.
- [14] B. M. Sicari, J. L. Dziki, B. F. Siu, C. J. Medberry, C. L. Dearth, S. F. Badylak, *Biomaterials* **2014**, *35*, 8605.
- [15] a) C. R. Nuttelman, M. C. Tripodi, K. S. Anseth, *Matrix Biol.* **2005**, *24*, 208; b) S. VandeVondele, J. Voros, J. A. Hubbell, *Biotechnol. Bioeng.* **2003**, *82*, 784; c) N. Wang, J. P. Butler, D. E. Ingber, *Science* **1993**, *260*, 1124.
- [16] F. G. Giancotti, E. Ruoslahti, *Science* **1999**, *285*, 1028.
- [17] a) I. G. Luzina, N. W. Todd, N. Nacu, V. Lockatell, J. Choi, L. K. Hummers, S. P. Atamas, *Arthritis Rheum.* **2009**, *60*, 1530; b) T. D. Zaveri, J. S. Lewis, N. V. Dolgova, M. J. Clare-Salzler, B. G. Keselowsky, *Biomaterials* **2014**, *35*, 3504.
- [18] a) E. A. O'Toole, *Clin. Exp. Dermatol.* **2001**, *26*, 525; b) Y. Nakayama, S. Kon, D. Kurotaki, J. Morimoto, Y. Matsui, T. Uede, *Lab. Invest.* **2010**, *90*, 881; c) T. T. Lee, J. R. Garcia, J. I. Paez, A. Singh, E. A. Phelps, S. Weis, Z. Shafiq, A. Shekaran, A. Del Campo, A. J. Garcia, *Nat. Mater.* **2015**, *14*, 352.
- [19] a) S. Gordon, P. R. Taylor, *Nat. Rev. Immunol.* **2005**, *5*, 953; b) H. Harrington, P. Cato, F. Salazar, M. Wilkinson, A. Knox, J. W. Haycock, F. Rose, J. W. Aylott, A. M. Ghaemmaghami, *Mol. Pharm.* **2014**, *11*, 2082.
- [20] S. R. Shin, H. Bae, J. M. Cha, J. Y. Mun, Y. C. Chen, H. Tekin, H. Shin, S. Farshchi, M. R. Dokmeci, S. Tang, A. Khademhosseini, *ACS Nano* **2012**, *6*, 362.
- [21] N. A. Peppas, Y. Huang, M. Torres-Lugo, J. H. Ward, J. Zhang, *Annu. Rev. Biomed. Eng.* **2000**, *2*, 9.
- [22] A. K. Blakney, M. D. Swartzlander, S. J. Bryant, *J. Biomed. Mater. Res., Part A* **2012**, *100*, 1375.
- [23] A. Mantovani, A. Sica, M. Locati, *Immunity* **2005**, *23*, 344.
- [24] a) E. Cassol, L. Cassetta, C. Rizzi, M. Alfano, G. Poli, *J. Immunol.* **2009**, *182*, 6237; b) M. Daigneault, J. A. Preston, H. M. Marriott, M. K. Whyte, D. H. Dockrell, *PLoS One* **2010**, *5*, e8668; c) A. L. Armstead, B. Li, *Int. J. Nanomed.* **2016**, *11*, 6195.
- [25] a) F. Y. McWhorter, T. Wang, P. Nguyen, T. Chung, W. F. Liu, *Proc. Natl. Acad. Sci. USA* **2013**, *110*, 17253; b) M. Bartneck, V. A. Schulte, N. E. Paul, M. Diez, M. C. Lensen, G. Zwadlo-Klarwasser, *Acta Biomater.* **2010**, *6*, 3864.
- [26] a) C. S. Chen, M. Mrksich, S. Huang, G. M. Whitesides, D. E. Ingber, *Science* **1997**, *276*, 1425; b) A. J. Engler, S. Sen, H. L. Sweeney, D. E. Discher, *Cell* **2006**, *126*, 677.
- [27] L. Beljaars, M. Schippers, C. Reker-Smit, F. O. Martinez, L. Helming, K. Poelstra, B. N. Melgert, *Front. Immunol.* **2014**, *5*, 430.
- [28] a) M. Genin, F. Clement, A. Fattaccioli, M. Raes, C. Michiels, *BMC Cancer* **2015**, *15*, 577; b) S. K. Biswas, E. Lopez-Collazo, *Trends Immunol.* **2009**, *30*, 475; c) C. Porta, M. Rimoldi, G. Raes, L. Brys, P. Ghezzi, D. Di Liberto, F. Dieli, S. Ghisletti, G. Natoli, P. De Baetselier, A. Mantovani, A. Sica, *Proc. Natl. Acad. Sci. USA* **2009**, *106*, 14978; d) J. Bi, X. Zeng, L. Zhao, Q. Wei, L. Yu, X. Wang, Z. Yu, Y. Cao, F. Shan, M. Wei, *Mol. Ther. Nucleic Acids* **2016**, *5*, e368.
- [29] a) A. D. Lynn, T. R. Kyriakides, S. J. Bryant, *J. Biomed. Mater. Res., Part A* **2010**, *93*, 941; b) A. D. Lynn, S. J. Bryant, *Acta Biomater.* **2011**, *7*, 123.
- [30] A. A. Tomei, C. Villa, C. Ricordi, *Expert Opin. Biol. Ther.* **2015**, *15*, 1321.
- [31] S. Bertholet, E. Tzeng, E. Felley-Bosco, J. Mauel, *J. Leukocyte Biol.* **1999**, *65*, 50.
- [32] J. T. Pesce, T. R. Ramalingam, M. M. Mentink-Kane, M. S. Wilson, K. C. El Kasmi, A. M. Smith, R. W. Thompson, A. W. Cheever, P. J. Murray, T. A. Wynn, *PLoS Pathog.* **2009**, *5*, e1000371.
- [33] a) Q. Zhang, Y. Wang, N. Zhai, H. Song, H. Li, Y. Yang, T. Li, X. Guo, B. Chi, J. Niu, I. N. Crispe, L. Su, Z. Tu, *Sci. Rep.* **2016**, *6*, 36160; b) A. C. Thomas, J. T. Mattila, *Front. Immunol.* **2014**, *5*, 479.
- [34] D. R. Schmidt, W. J. Kao, *J. Biomed. Mater. Res., Part A* **2007**, *83*, 617.
- [35] V. P. Yakubenko, N. Belevych, D. Mishchuk, A. Schurin, S. C. Lam, T. P. Ugarova, *Exp. Cell Res.* **2008**, *314*, 2569.
- [36] B. Eckes, M. C. Zweers, Z. G. Zhang, R. Hallinger, C. Mauch, M. Aumailley, T. Krieg, *J. Invest. Derm. Symp. P* **2006**, *11*, 66.
- [37] J. D. Humphrey, E. R. Dufresne, M. A. Schwartz, *Nat. Rev. Mol. Cell Biol.* **2014**, *15*, 802.
- [38] a) V. P. Lehto, T. Hovi, T. Vartio, R. A. Badley, I. Virtanen, *Lab. Invest.* **1982**, *47*, 391; b) A. Taylor, W. Tang, E. M. Bruscia, P. X. Zhang, A. Lin, P. Gaines, D. Wu, S. Halene, *Blood* **2014**, *123*, 3027.
- [39] D. Y. Vogel, P. D. Heijnen, M. Breur, H. E. de Vries, A. T. Tool, S. Amor, C. D. Dijkstra, *J. Neuroinflammation* **2014**, *11*, 23.
- [40] H. M. Rostam, P. M. Reynolds, M. R. Alexander, N. Gadegaard, A. M. Ghaemmaghami, *Sci. Rep.* **2017**, *7*, 3521.
- [41] M. R. Fernando, J. L. Reyes, J. Iannuzzi, G. Leung, D. M. McKay, *PLoS One* **2014**, *9*, e94188.
- [42] D. E. Heath, A. R. Sharif, C. P. Ng, M. G. Rhoads, L. G. Griffith, P. T. Hammond, M. B. Chan-Park, *Lab Chip* **2015**, *15*, 2073.
- [43] M. L. Albert, S. F. Pearce, L. M. Francisco, B. Sauter, P. Roy, R. L. Silverstein, N. Bhardwaj, *J. Exp. Med.* **1998**, *188*, 1359.
- [44] a) T. A. Ferguson, J. Herndon, B. Elzey, T. S. Griffith, S. Schoenberger, D. R. Green, *J. Immunol.* **2002**, *168*, 5589; b) W. R. Heath, F. R. Carbone, *Annu. Rev. Immunol.* **2001**, *19*, 47.
- [45] a) H. J. Anders, M. Ryu, *Kidney Int.* **2011**, *80*, 915; b) S. C. Huen, L. G. Cantley, *Pediatr. Nephrol.* **2015**, *30*, 199; c) S. D. Ricardo, H. van Goor, A. A. Eddy, *J. Clin. Invest.* **2008**, *118*, 3522.
- [46] a) D. M. Faulk, R. Londono, M. T. Wolf, C. A. Ranallo, C. A. Carruthers, J. D. Wildemann, C. L. Dearth, S. F. Badylak, *Biomaterials* **2014**, *35*, 8585; b) M. T. Wolf, C. L. Dearth, C. A. Ranallo, S. T. LoPresti, L. E. Carey, K. A. Daly, B. N. Brown, S. F. Badylak, *Biomaterials* **2014**, *35*, 6838.
- [47] E. F. Plow, T. A. Haas, L. Zhang, J. Loftus, J. W. Smith, *J. Biol. Chem.* **2000**, *275*, 21785.
- [48] A. I. Van Den Bulcke, B. Bogdanov, N. De Rooze, E. H. Schacht, M. Cornelissen, H. Berghmans, *Biomacromolecules* **2000**, *1*, 31.